Journal of The Electrochemical Society, **160** (6) F636-F644 (2013)
0013-4651/2013/160(6)/F636/9/$31.00 © The Electrochemical Society

Oscillation of PEFC under Low Cathode Humidification: Effect of Gravitation and Bipolar Plate Design

Daniel G. Sanchez,[a,z] Alfredo Ortiz,[b] and K. Andreas Friedrich[a,*]

[a]*Deutsches Zentrum für Luft und Raumfahrt (DLR), Institut für Technische Thermodynamik, 70569 Stuttgart, Germany*
[b]*Departamento Ingeniería Química y QI. ETSII y T, Universidad de Cantabria, Santander, Cantabria 39005, Spain*

Oscillatory fluctuations of a single proton exchange membrane fuel cell appear upon operation with a dry cathode air supply and a fully humidified anode stream. Periodic transitions between a low- and high-current operation point of the oscillating state due to the balance of drying and wetting processes in combination with water transport have been observed previously; however, several new aspects have been investigated in the present study, providing insight into the initiation processes. Oscillations are present under both galvanostatic and potentiostatic conditions, and it is demonstrated that the transitions involve local membrane drying through the comparison of impedance data with current density distributions. The oscillations are caused by periodic flow type changes from one- to two-phase flow in the anodic channels of the flow field. It has been observed that cell orientation with respect to Earth's gravity field affects the liquid water distribution in the anodic flow channels and, thus, also affects the oscillatory behavior of the cell performance. When comparing cell performance oscillations with a five-channel serpentine flow field to a cell with a one-channel serpentine flow field, the oscillating performance behavior is observed to also be affected by the gas velocity within an anodic flow channel.
 [DOI: 10.1149/2.091306jes]

Manuscript submitted December 20, 2012; revised manuscript received March 20, 2013. Published April 4, 2013.

Polymer electrolyte membrane fuel cells (PEMFCs) are expected to play an important role in the future for energy supply when hydrogen is available as a fuel. As electrochemical energy converters, these fuel cells enable the direct and efficient conversion of hydrogen energy into power for stationary, portable and automobile applications. An efficient and reliable operation of fuel cells requires a comprehensive understanding of the underlying physicochemical processes.[1,2] Water management represents one of the main challenges in the design and operation of PEMFCs. Maintaining proper membrane humidity is one of the key requirements to reach optimum performance, which is especially necessary for automotive applications.[3–6] Water management is generally provided through external pre-humidification of the reactant gases and by the water generated in the cell reaction. However, in some applications, the extra size and weight of the humidifier should be avoided.[7] Imbalance between production and evaporation rates can result in either flooding of the electrodes or membrane dehydration, both of which severely limit fuel cell performance and fuel cell life.[8–10]

Thus, water management has been the main focus of study for numerous groups in recent years. The mechanisms of water transport in the ionomer of the membrane and catalyst layer (CL) involves diffusion, electro-osmotic drag by protons from the anode side to the cathode and hydraulic permeation. In the pores of the gas diffusion layer (GDL) and the catalyst layer and in the flow channel, the transport of water vapor involves diffusion and convection. The capillary force also plays an important role in liquid water transport in the pores of the GDL and CL. Knudsen diffusion can be neglected in the pores of the substrate GDL and in the flow channel but needs to be considered in the much smaller pores of the CL and the microporous layer (MPL). Among the mechanisms of water transport, electro-osmotic drag and back diffusion are functions of the fuel cell temperature, current density and membrane water content (humidity). Phase change processes occur until the equilibrium states are achieved. However, whether phase equilibriums of water exist remain debated because of the presence and arbitrary transport of liquid water, especially in the heterogeneous structures of the CL and GDL.[11–15]

Several experimental works have described water management and the self or partial humidification operation without external humidification, demonstrating stable operation states in some cases.[16–18] Additionally, numerous studies have presented theoretical models using computational fluid dynamics (CFD) software to describe water transport in PEMFCs, through which the instability of the fuel cell system could be explained.[19–21] Simulation results have shown that a cathode humidifier is necessary to maintain a high water content of the fuel cell membrane, whereas an anode humidifier is not needed. The performance of the humidifier is affected by the inlet air and water conditions, such as the flow rate, temperature and relative humidity.[22–25] Experimental and theoretical studies have revealed nonlinear responses, such as multiple steady states as well as periodic oscillations. Studied oscillations in PEMFCs can result from either poisoning effects of the catalysts[26] or complex water management. The study of the current oscillations under low cathode hydration has been the focus of several research groups recently, with the aim of understanding the variables that control the phenomenon and its origin.[11,27–29]

To achieve a better understanding of the electrochemical processes in PEMFCs and to investigate the effects of operating conditions on the local performance, a variety of locally resolved current density distribution mapping techniques have been developed.[6] Among these techniques, segmented fuel cell technology is one of the important technologies applied for the in-situ detection of the fuel cell system. Sánchez et al.[28] have presented current density distributions for drying changes with high and low cell currents at distinct times, indicating a propagating active area with defined boundaries with a downward transition period that strongly depends on the operation conditions.

The oscillatory behavior of the cell performance induced by large humidity gradients from the wet anode to dry cathode air is significant as it allows us to understand and evaluate some of the processes related to the management of water in PEMFCs. In particular, there are interesting features in the oscillation that have the potential for advancing the understanding of water interaction in the cell: (i) the downward transition associated with dehydration of the membrane, which has a considerable stability and can be studied using in situ techniques (e.g., electrochemical impedance spectroscopy (EIS) in segments); (ii) a transient high current operation point that corresponds to the steady state of the cell under optimum hydration conditions; and (iii) a characteristic upward transition time that does not depend on operation conditions for a membrane system.

The rate of transition between the high to low level (corresponding to a change from the hydrated to dehydrated cell) depends markedly on the drying conditions and the amplitude of the oscillations, which permits direct comparison of the dehydration degree of the cell under the operational conditions and the design selected. However, the high level indicates the full performance potential of the cell at any time and can be used for determining degradation rates. Although the controlling mechanism of transition from the low- to high-current state has not been completely clarified, it is clear that the mechanism is associated with the presence of liquid water in the anode channel. Some

*Electrochemical Society Active Member.
[z]E-mail: Daniel.GarciaSanchez@dlr.de

models have been proposed to describe this transition, as it is analyzed in the work reported by Nazarov et al.,[30] which does not include local resolution, or in the recent work by Sanchez et al.,[28] which proposes a simple model to describe the drying process. This study relates the amplitude of the oscillations to the amount of H_2O in the membrane. It is known that the transition from low to high currents, often called ignition in the literature, depends strongly on anode local processes, as was discussed by Atkins et al.[27] and confirmed by in situ current density distribution measurements.[11]

The flow field structure, which is integrated into bipolar plates, is also an important design component because it serves as a fuel or air distributor and as a current collector. This structure affects the reactant transport, water management and reactant utilization efficiency. The flow field channel design is especially important for water management inside the fuel cells because the design determines water transport within the cell. An appropriate flow field design not only enhances reactant transport rates in the flow channel and gas diffusion layer (GDL) before reaching the catalyst layer (CL) for the reaction but also improves liquid water removal.[31–33] Many studies analyzing the effects of various flow channel designs and rib cross-sectional areas, such as serpentine channels, multiple channels in parallel and interdigitated channels, on the cell performance have demonstrated that narrower channels with wider rib spacing resulted in higher performance.[33,34]

In this paper, we present several advances in the understanding of the oscillatory fluctuations under dry cathode air supply and wet anode hydrogen flow conditions. First, a comparison between the galvanostatic and potentiostatic measurements in combination with variations of anode humidity and cathode flows provides insight into their effects on the oscillatory amplitude and frequency. Second, a clear correlation of the transition from low to high performance with the existence of liquid water in the anode and the importance of forced water convection is demonstrated. The measured effect of the oscillatory behavior on the orientation of the PEMFC with respect to Earth's gravity field further supports this interpretation. Moreover, we compare the effect of the flow channel geometry on the performance with a five-channel serpentine flow field and a cell with a single-channel serpentine flow field. Different rib widths for the single serpentine flow field are investigated. This study provides the essential insight necessary for a future complete model description of PEFC oscillations.

Experimental

The dynamic response of polymer electrolyte fuel cells was investigated on single cells with an electrode area of 25 cm^2 at in-house-developed testing stands of the German Aerospace Center (DLR). The test bench, controlled by programmable logic controllers (PLCs), allows automatic control of the input and output conditions, such as the pressure, temperature, flow rate of gases and humidity of reactants. The gas mass flow rates (air and H_2) were controlled through the test station and could be varied between 0 and 500 mL min^{-1} on the anode side and between 0 and 2000 mL min^{-1} on the cathode side. The pressure was fixed at 1500 mbar for the experiment. The reference operating conditions are summarized in Table I. Co-flow and counter-flow configurations of the flow fields were used in the present study. The relative humidity of the inlet gases was controlled through water-filled, heated sparger bottles. These testing stands have the possibility to by-pass the bubblers and introduce dry gases into the cell. A relative humidity (RH) of approximately 5% was applied to the cathode side under dry conditions, which was accomplished by introducing ambient (20°C) gas using the bubbler by-pass.

Table I. Experimental conditions.

Potentiostatic mode: 600 mV
Galvanostatic mode: 15 A
Flows:
- Anode (H_2): 209 mL/min
- Cathode (Air): 664 mL/min

Bubbler Anode temperature 80°C
Cell temperatures: 80°C
Pressure: 1.5 bar
Relativity humidity:
- Anode (H_2): 100%
- Cathode (Air): ca. 5%

Commercial electronic loads were used in the test stands and for the measurements. Here, the galvanostatic and potentiostatic modes were used, meaning that the cell current or voltage was kept constant, whereas the corresponding voltage or current changed with time by adjusting itself to the power generation. Electrochemical impedance spectroscopy measurements were performed using an electrochemical station (Zahner) in galvanostatic and potentiostatic mode with an amplitude of 10 mV in a frequency range of 100 mHz to 500 Hz.

The active area of the cell was 25 cm^2 (5 cm × 5 cm), and the membrane electrode assembly (MEA) was a commercial Nafion-111-IP with an anode and cathode Pt loading of 0.3 mg_{Pt} cm^{-2} on each side (Ion Power Inc. Company). For the GDL, a SGL Group Sigracet 35 BC was used for all measurements.

An important aspect of the performance measurement is the flow field used. For this study, three different DLR plates, specifically fabricated for this study, were used galvanized stainless steel bipolar plates were used to study their effects on the oscillatory phenomena. The characteristics of the different bipolar plates used include the following:

(A) Single serpentine anode: 1-mm channel width; 1-mm rib width/Single serpentine cathode: 1-mm channel width; 0.5-mm rib width
(B) Single serpentine anode: 1-mm channel width; 1-mm rib width/Single serpentine cathode: 1-mm channel width; 1-mm rib width
(C) Five serpentine anode: 1-mm channel width; 1-mm rib width/Five-fold serpentine cathode: 1-mm channel width; 1-mm rib width.

Most in situ methods used in fuel cells are integral and, therefore, do not allow a locally resolved analysis of the cell. However, it is important to obtain local information as inhomogeneous distribution of reactants and products often occurs depending on the operating conditions. In the present experiments, locally resolved current density measurements in a single cell were performed to gain insight into the nature of the oscillating fluctuations. The configuration for the single serpentine flow field is illustrated in Figure 1. The channel cross-section is 0.1 cm × 0.1 cm.

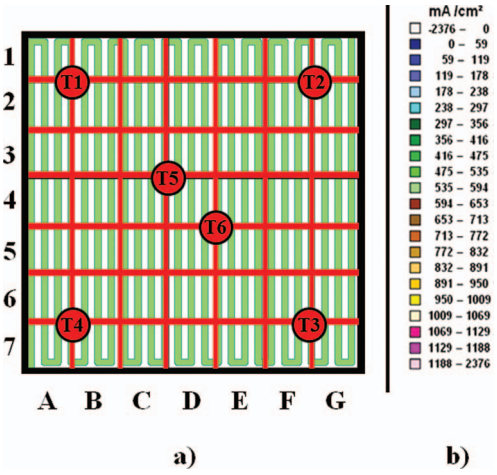

Figure 1. Single serpentine segmented cell design: (A) segment distributions with T1-T6 indicating the location of the temperature sensors and (B) color code for current density ranges.

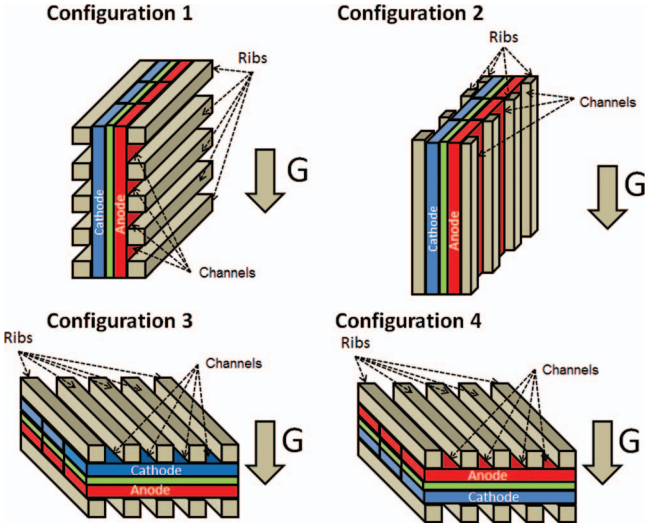

Figure 2. The four orientations used to study the effect of gravitation on cell performance.

A segmented bipolar plate based on printed circuit board (PCB) technology with integrated temperature sensors was used in the single cell to investigate the locally resolved current density distributions.[35,36] The temperature sensors are needed for resistance calibration and to maintain an isothermal measurement; the PCB board was introduced at the anode side. Other groups have also developed methods and tools for current density distribution measurements.[37–39]

The present work also demonstrates the effect of the orientation of the bipolar plates on the oscillatory phenomena to evaluate the effect of the gravity field. Four different configurations, as illustrated in Figure 2, are used to study the effect of gravity on the cell performance.

1. Configuration 1 has the MEA perpendicular to the Earth's surface, and the channels are parallel to this surface.
2. Configuration 2 has the MEA and the channels perpendicular to the Earth's surface plane.
3. Configuration 3 has the MEA parallel to the surface plane with the cathode up and the anode down.
4. Configuration 4 has the MEA parallel to the surface plane with the cathode down and the anode up.

Most of the experiments were performed using configuration 1. Only the results presented in Figures 12 and 14 correspond to different configurations.

Results and Discussion

This work is intended to complement previous studies that focused on the oscillatory response of a single proton exchange membrane fuel cell under pronounced humidity differences between the anode (wet) and cathode (dry) compartments. Insight into the transitions between high- and low-current operation points is obtained based on current density distributions at distinct times, indicating a propagating active area with defined boundaries. We aim to contribute to the understanding of the phenomena associated with water management within the fuel cell.

Even though the conditions of normal stack operation vary considerably compared with the conditions under which oscillatory fluctuations appear, several groups have been interested in this phenomena.[11,27,29] The reason for this interest is that water transport plays a crucial role in fuel cell performance and reliable operation. However, water transport in a fuel cell depends on the flow rate dependent influx and removal, pressures, electroosmotic drag, the reaction rate and back diffusion. Therefore, the complex effect of water transport on current voltage curves cannot be currently modeled in an unambiguous way. The appearance of oscillations under humidity gradient conditions opens the path to a much better understanding of water transport properties due to the distinct effects of transient behavior on operation conditions and the possibility of experimentally validating two-phase flow models with high accuracy. A model that accurately describes the oscillatory behavior will have superior predictive potential for fuel cell operation in general.

In principle, oscillatory behavior requires two states with stability at the same operation conditions of the cell. In our case, the driving force for the oscillation is the humidity gradient from the anode to cathode, which is responsible for the two opposing processes: the drying process from the cathode side, which reduces performance, and the wetting process from the anode side, which compensates for the drying effect. We demonstrate that a minimum water quantity on the anode side is needed to overcome the drying effect. The balance between these two processes determines the minimum performance level, the amplitude and the frequency associated with the oscillatory behavior. One factor is the minimum performance level, which is determined by the threshold amount of water provided at the anode as demonstrated by Sanchez et al.[11] Without this minimum anode humidity, the oscillatory behavior is not perceived. Other characteristic quantities are the oscillation amplitude and frequency. Oscillations have been reported for cathode relative humidities from approximately 5–70% and anode humidities from approximately 75–135%. The humidity gradient is as important as the pressures and gas flow rates.

The amplitude of the oscillations are highly related to the local amount of H_2O in the membrane, as reported in previous works. In Figure 3, a comparison of the oscillatory behavior for (a) galvanostatic and (b) potentiostatic operation is provided, and the corresponding current density distributions for a counter-flow configuration with the operation parameters of Table I are presented. Oscillations in electrochemical systems are related to the negative impedance characteristics of the faradaic processes at the electrode and are normally observed under strictly galvanostatic or potentiostatic conditions. Therefore, it is of interest that periodic transitions between a low- and high-current operation point of the oscillating state are observed for both operation

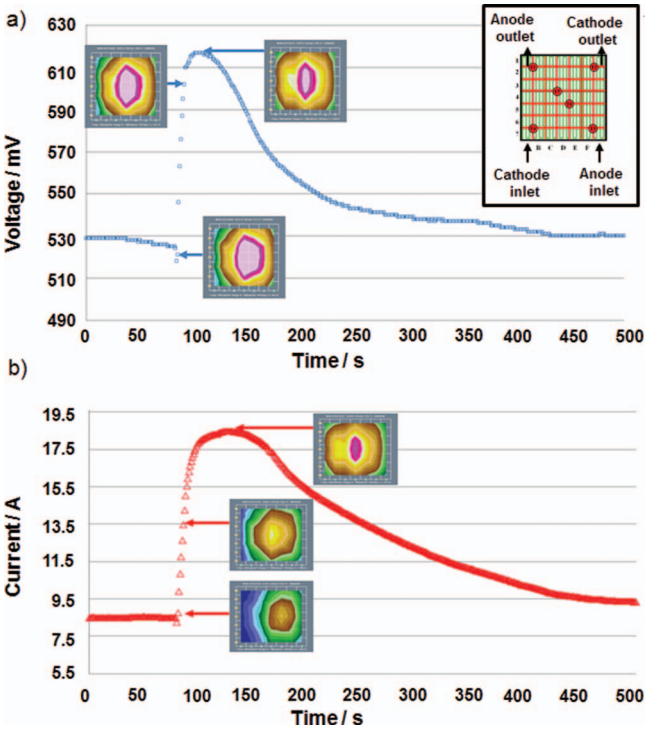

Figure 3. (A) Galvanostatic operation at 20 A and (B) potentiostatic operation at 600 mV and the corresponding current density distributions for a counter-flow configuration with the operation parameters of Table I are presented.

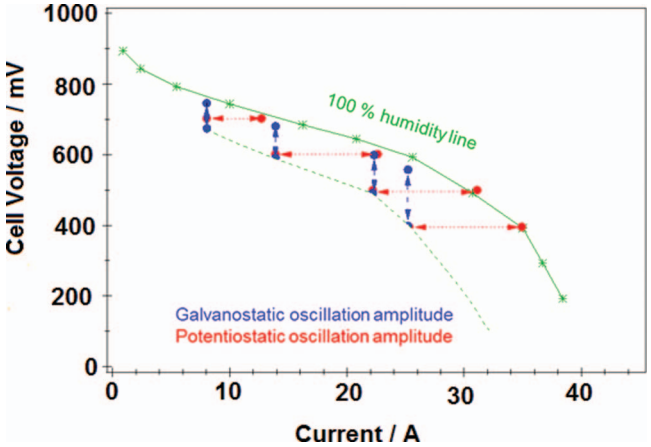

Figure 4. Comparison of the oscillation amplitudes of galvanostatic (dotted red line) and potentiostatic operation (broken blue line) with the current voltage curve at 100% RH (stoichiometric ratio: 1.5 (H_2) and 2 (Air)).

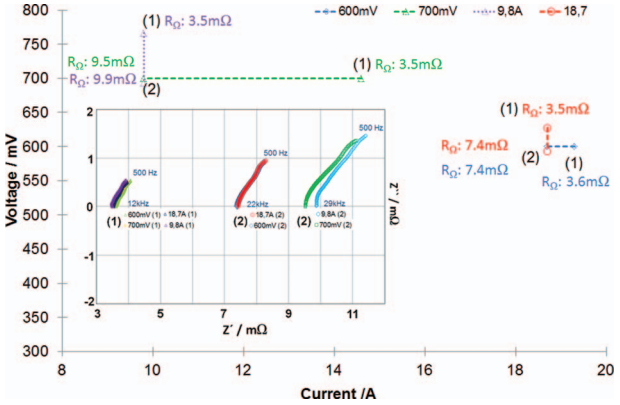

Figure 5. Comparison of the oscillation amplitudes and membrane resistances of galvanostatic and potentiostatic operation: (1) wet with 100% RH on both sides (2) dry with 100% RH at the anode and 5% RH at the cathode for the low performance level. 80°C cell temperature, 1.5 bar pressure, 209 mL/min anode flow; 664 mL/min cathode flow.

modes. The transition time of 20–25 s for the change from the low to the high operation is fast and does not depend on the operating parameters, while the downward transition depends strongly on the operating conditions. The current density distributions at distinct times for high and low currents indicate that the transitions are associated with a propagating active area with defined boundaries for both operation modes under this flow configuration. The observations agree with the assumption of a liquid water reservoir at the anode with a downward transition period depending on the operation conditions. The high-current operation possesses a high electro-osmotic drag and a high permeation rate (corresponding to liquid-vapor permeation), leading to a large water flux to the cathode. Subsequently, the liquid reservoir at the anode is consumed, leading to drying of the anode. The system establishes a new quasi-stable operation point associated with a low current, low electro-osmotic drag coefficient, and low water permeation (corresponding to vapor-vapor permeation). When liquid water is formed at the anode interface, a fast transition to the high-current operation occurs after a period of time due to the flooding effect leading to blockage of channels. Figure 4 compares the amplitudes determined from the oscillations in galvanostatic and potentiostatic operation at identical operation conditions for 100% RH on the anode side and approximately 5% RH on the cathode side with the current voltage curve determined from this cell at constant 100% RH conditions. It can be observed that both operation modes exhibit the same limiting high or low performances within measurement error, which correspond to these operation conditions. It can be concluded that for both operation modes, the upper limit of performance corresponds to the full (optimum) humidification of the cell, whereas the lower operation point corresponds to an extrapolated stable current voltage curve for reduced humidity conditions. In this case, the comparison is made at constant stoichiometries of the anode ($\lambda_{H2} = 1.5$) and cathode ($\lambda_{Air} = 2$), which implies that the flow rates vary along the current voltage curves. Next, we will discuss measurements where the flow rate is kept constant to maintain the same water influx and removal rates.

Electrochemical impedance spectroscopy (EIS) measurements.— To determine the ohmic cell resistances, EIS measurements at high frequencies (over 500 Hz) were performed under dry cathode conditions. Due to the oscillations, it was not possible to measure the entire EIS spectrum because the requirement of stationary conditions limits the duration of the measurement. Differences in the membrane resistances were observed for different humidity conditions using both the galvanostatic and potentiostatic modes. In particular, we studied 100% RH on both sides without oscillations (1) and 100% RH on the anode and 5% RH on the cathode side (2) for the low level response. The results are presented in Figure 5. The gas flows were kept constant for all the experiments to maintain unchanged convection processes. The variation of the ohmic resistances from wet (1) to dry (2) conditions, which are mainly determined by the membrane resistance, is similar in the measurements made in the galvanostatic and potentiostatic mode. This finding demonstrates the equivalence of these two operation modes in relation to these phenomena. From the measured values, it is clear that a membrane drying process is involved in the wet-dry transition because the contact resistance remains unchanged during the measurements. Interestingly, the low performance operation resistance exhibits variations depending on the voltage or the current level. This dependence is associated with different water transport and generation rates, which lead to differences in the active cell area, as discussed in the next section.

Effect of active cell surface on membrane resistance.— A previous study[11] reported a correlation of the membrane-resistance changes associated with the transition between high- and low-performance levels. Membrane resistance is inversely proportional to the membrane water content. To elucidate this correlation, three different conditions and their measured ohmic resistances by EIS are compared in Figure 6. A comparison of the resistances at a cell voltage of 600 mV for a markedly different current density distribution is presented. The

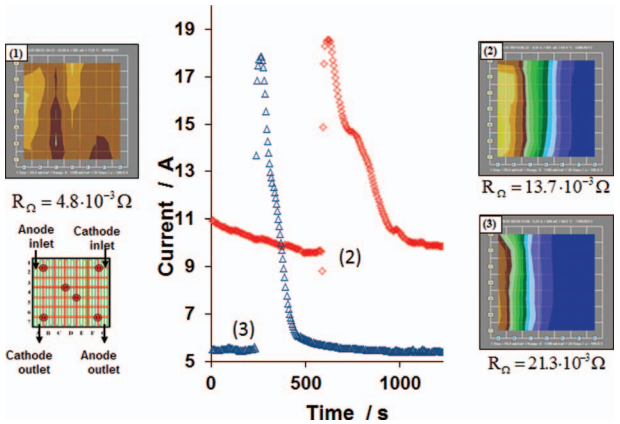

Figure 6. Membrane resistances and current density distributions; 600 mV cell voltage, 70°C cell temperature (1) 100% RH cathode humidification, 100% RH anode humidification (2) Cathode humidification of approximately 7%, anode humidification of RH > 100%, anode flow of 261 mL/min, cathode flow of 832 mL/min (3) Cathode humidification of approximately 7%, anode humidification of RH > 100%, anode flow of 261 mL/min, cathode flow of 1662 mL/min.

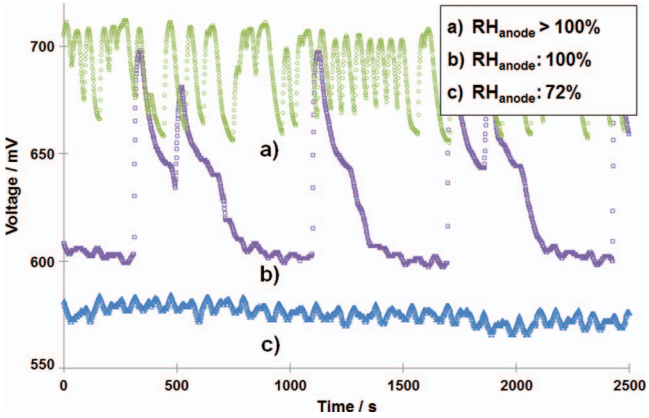

Figure 7. Effect of the anode RH on the oscillation behavior, anode RH of: 72% (triangles), 100% (circles) and 137% (diamonds); other parameter values according to Table I conditions.

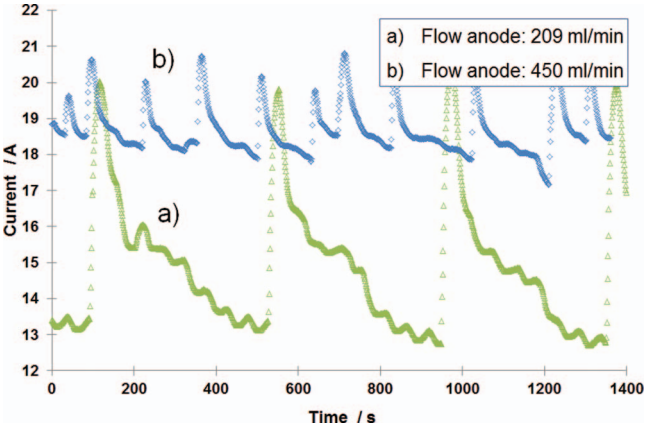

Figure 8. Effect of the anode flow on the oscillations. Anode flow values: 209 mL/min (triangles), 450 mL/min (diamonds), potentiostatic mode, other parameter values according to Table I conditions.

reference operation is the cell response at a stable and high performance with high humidity gases (100% RH), as shown in Figure 6 (1). A uniform current density distribution with high values is observed with an ohmic resistance of 4.8 mΩ. For a reduced RH of approximately 7% at two different cathode air flows with otherwise identical conditions, performance transitions are observed in Figure 6 (2), (3). The current density distributions in Figure 6 (2), (3) exhibit differences in the active areas that are related to the drying effects of the cathode flows. For the highest cathode flow (3), the current density distribution exhibits only a small active area at the left side of the image. The ohmic resistances, dominated by the membrane resistance under these conditions, exhibit relatively high values of 13.7 mΩ (2) and 21.3 mΩ (3) for the dry conditions. The reciprocal resistance values correlate well with the active surface area when comparing the wet conditions (1) and dried conditions (2) and (3) (approximately 54% higher in (3) than for (2) for half the surface area). This observation supports the interpretation that the current density distribution provides direct information about active area of the membrane.

It is interesting to investigate the effect of different RH values at the anode side to determine the importance of the driving force of the humidity gradient for the oscillations. The measurements at three different RHs at the anode are presented in Figure 7 for galvanostatic operation. These experiments demonstrate that the "ignition" transition from low to high current levels requires a minimum value of RH on the anode side to occur. With RH values at the anode lower than 72% (triangles), ignitions were not observed. At a RH of 72%, the humidity gradient is low, and the water amount in the cell is also reduced, which leads to small fluctuations (very small amplitude) at low performance of the cell. Increasing the RH on the anode side from 72% to 100% (squares) corresponds to an additional 22% in the net amount of water in the anode, which induces the ignition transition, leading to pronounced voltage amplitudes and characteristic times of approximately 400 s between the low-performance regions, which are the more durable conditions of the cell. For these conditions, the high-performance operation point tends to appear as duplets, and the amplitude is approximately 100 mV between the low- and high-performance points. Increasing the anode RH from 100% to 135% (circles) involves a 40% addition to the net water amount in the anode side and results in a higher ignition frequency. Now, the characteristic time between low operation performances is only in the range of 50–80 s, and the amplitude is reduced to 50 mV. The high-performance operation seems to be more stable than the low-performance operation point. With this series, it can be concluded that the amplitude is maximized after reaching a threshold value and diminishes with increasing water content at the anode.

To further analyze the relation between the water in the anode and the ignition transition, the anode flow effect on the oscillation behavior is examined. Figure 8 demonstrates that at higher flows, the oscillation frequency increases, which is consistent with the data shown in Figure 7. The frequency increase can be associated with an increasing amount of water at the anode side. For this particular experiment, the resulting water mass is 44% higher for the higher flow rate of 450 mL/min compared with that for the 209 mL/min flow rate.

Increasing the amount of water in the anode inlet can counteract the drying process in the cell from the cathode side, which results in a more stable response with increased performance (with a decrease in the oscillating amplitude). This result is consistent with previous works.[11,29] The measurements in Figures 7 and 8 demonstrate that the net water amount in the anode inlet reduces the amplitude of the oscillations. Such a trend is considered to arise from the inhibition of the drying process at the anode side of the cell.

At this point, it becomes useful to study the differences between the proposed methods to counteract the drying process: (1) using a large RH value or (2) applying high flows at the anode side. With this objective, the net amount of water in the anode was kept constant in both experiments, as observed in Figure 9. Using a high flow value in the first configuration and a large RH for the other configuration in this figure, higher flows are observed to generate a stable response and uniform current density distributions. In contrast, with the same net amount of water in the anode but with higher values of RH, unstable responses are obtained, with voltage drops and deactivation of current density distributions in some areas near the cathode inlet, associated with the drying process. It is clear from these measurements that increasing flow rates is a superior strategy for homogenizing current

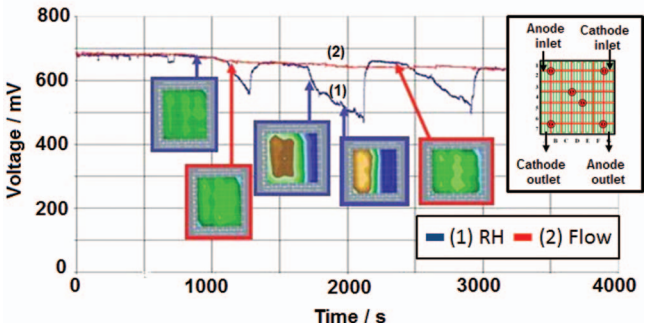

Figure 9. Counter flow, one serpentine anode and four serpentine cathode flow fields, 10 A galvanostatic mode, T_{cell}: 70°C, pressure: 1.5bar, RH cathode: approximately 7%, cathode flow: 330 mL min^{-1}, net amount of water in anode: 3 g/h (1) 159% anode RH (blue), (2) 100% anode RH (red), (1) 100 mL min^{-1} anode flow (blue), (2) 209 mL min^{-1} anode flow (red).

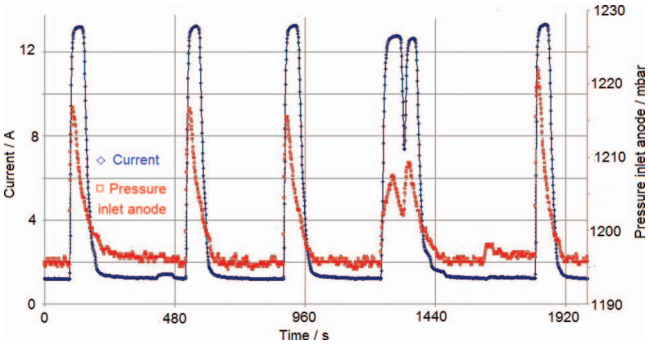

Figure 10. Relationship between pressure peaks and peaks of current (corresponding to ignition transitions).

density distributions. This conclusion may be of general validity and will be tested in other configurations.

For these experimental conditions with a completely dry cathode, the amount of water in the anode inlet determines the limiting performances for the oscillatory behavior. The stability differences between these operation conditions, which are equivalent regarding the water content, indicate that convective mass transport is of special importance for minimizing inactive cell areas.

Next, the relation between H_2O in the liquid phase in the anode channel and the ignition transition of low to high performance will be discussed. In Figure 10, the time evolution of current (blue diamonds) and inlet anode pressure (red squares) for oscillatory measurements are compared. A complete time correlation between both variables can be observed. Pressure peaks are related to the presence of two-phase water (vapor and liquid) in the anode channel as liquid water blocks the single serpentine channel and concurrently leads to pressure inlet peaks. The pressure peak apparently is concurrent with the ignition transition.

To correlate the two-phase water presence in the anode channel to the ignition transition, it is necessary to monitor the pressures at different positions in the cell, as displayed in Figure 11, where the time evolution of the cell pressures can be observed. The synchronized

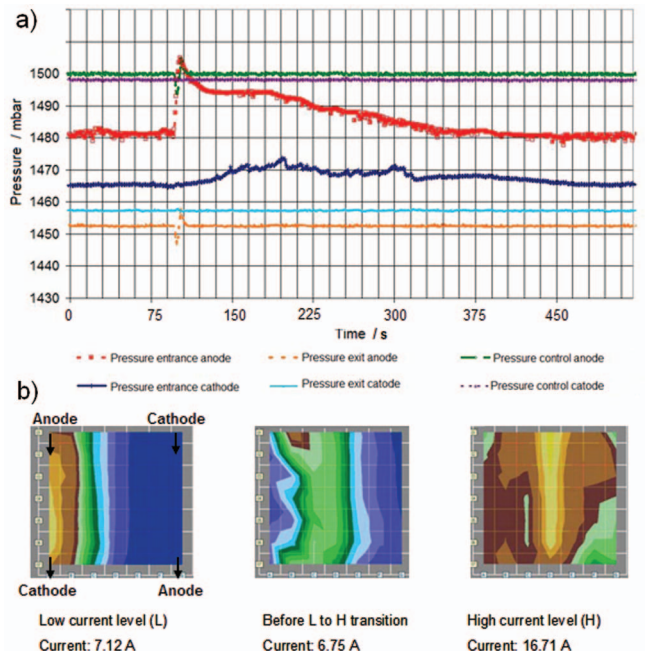

Figure 11. (A) Pressures and (B) current density distributions in the cell during the ignition event, low to high performance transition.

pressure increase in the anode inlet (red squares) and the start of the transition toward high performance is again evident, while pressure decreases somewhat at the anode outlet (orange line). This behavior is consistent with the already proposed blocking of liquid water in the anode channel, which leads to a pressure increase in the inlet region and may lead to a forced convection of water into the membrane. It may be concluded that this partial obstruction of the serpentine channel is the result of the two-phase fluid occurrence in the anode channel as demonstrated by Ly et al.[40] The liquid water can be produced spontaneously by condensation as described by Wang et al.[41] Interestingly, a pressure increase is also observed at the cathode inlet with a delay of approximately 600 - 700 ms. Liquid water also appears at the cathode channel[42] due to the ignition transition at the anode side, confirming the assumption of forced water convection through the cell. In addition, the current density distribution monitored near the ignition transition exhibits a prominent change from the current density distribution at the extremes of performance (see Figure 11B). At the ignition transition, higher performance is observed in the middle of the cell, and the area of high performance to the left shows reduced activity. This finding indicates that blocking the channel leads to fuel stagnation even in this formerly highly active area.

Effect of cell orientation on transient response.— Once the existence of liquid water in the anode has been related to the appearance of ignition (Figures 3-11), it seems reasonable to also expect an effect of gravity on the oscillatory phenomenology because it may contribute to the accumulation of H_2O in the liquid state in the channel.[43] Therefore, different orientations of the gravity field are compared regarding their effect on the oscillations in the cell. The investigated orientations correspond to the configuration presented schematically in Figure 2.

First, configurations 1 and 2 shown in Figure 2 are compared. The analysis begins by keeping the cell in a vertical position (MEA perpendicular to the ground plane) and comparing the use of channels parallel to the ground (configuration 1) with the use of perpendicular channels (configuration 2). For both configurations, the gravity force is perpendicular to the water flow in the membrane; however, we can expect a facilitated removal of water in configuration 2, leading to a reduced channel-blocking tendency. Hence, a pronounced difference in the oscillatory behavior can be observed in Figure 12. The current density distributions for configuration 1 exhibit dramatic changes in the active surface area for the two performance levels. In contrast, in configuration 2, the differences in the current density distribution can be considered marginal. Only some smaller active spots appear for the higher performing operation points. Interestingly, the low performance current density distribution for configurations 1 and 2 are almost indistinguishable.

According to the work published by Lu et al.,[44] a design corresponding to configuration 1, with channels parallel to the surface plane, enhances H_2O accumulation in the liquid state inside the

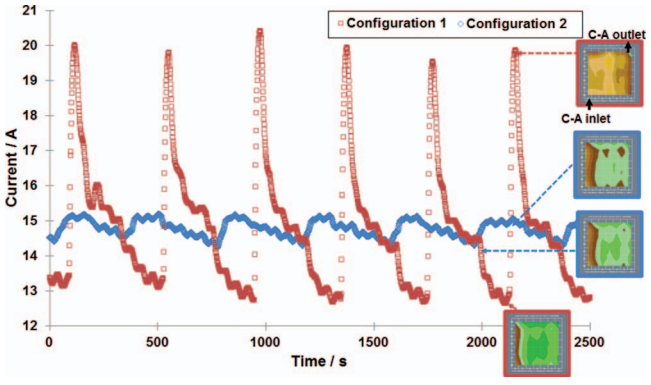

Figure 12. Channel orientation effect in a cell with a MEA perpendicular to the surface plane, configuration 1 (squares) vs. configuration 2 (diamonds) under the conditions of Table I in potentiostatic mode.

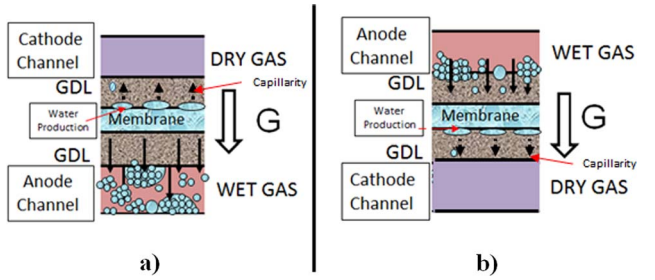

Figure 13. Cell structure schematic of (A) configuration 3 and (B) configuration 4.

channels. It has been argued above that this condition has a significant effect on prominent ignition appearance. This process can be observed in Figure 12 (squares symbols). In comparison, for configuration 2, with channel directions perpendicular to the ground plane (diamonds), the cell response exhibits a dramatically reduced ignition feature. For some of the experimental conditions applied under this configuration, ignition occurrences have been observed but always with a lower frequency than the one observed for configuration 1. Therefore, we can correlate a decrease in the liquid H_2O accumulation in the channel, as reported by Lu et al.,[44] to the absence of real ignition transitions in configuration 2.

In addition to the effect of the channel orientation on the oscillatory phenomenon, it is interesting to evaluate the effect of gravity on the MEA side orientations, comparing configurations 3 and 4.

In configuration 3, the well-hydrated anode is placed at the bottom of Figure 13a. In this manner, liquid water accumulation in the anode channel is enhanced, and we expect an increase in the ignition occurrences from the earlier observations. This configuration also results in reduced H_2O flow from the channel to the membrane, which is associated with reduced wetting of the membrane.

In configuration 4, the anode is placed on top, enhancing the water flow from the anode channel to the membrane, as observed in Figure 13b. This situation produces two different effects: on one hand, this enhancement contributes to the hydration of the membrane and, on the other hand, the enhancement reduces the liquid water accumulation in the anode channel. This effect is exacerbated by the hydrophobic properties of the GDLs, which should facilitate the water removal, thereby reducing the ignition occurrences.[45] This expectation was confirmed in the measurements presented in Figure 14, where configuration 3 exhibits prominent transitions with uniform current density distributions in the high performance level. A comparison between the low performance levels in configurations 3 and 4 reveals similar current distributions but with slightly smaller

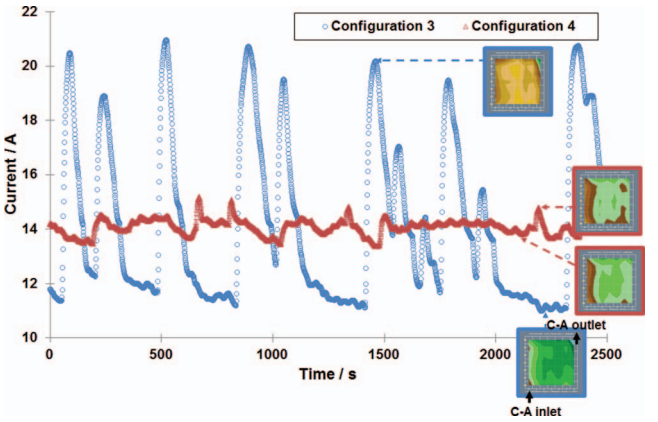

Figure 14. Cell orientation effect with MEAs parallel to the surface plane, configuration 3 (circles) vs. configuration 4 (triangles) under the conditions of Table I in potentiostatic mode.

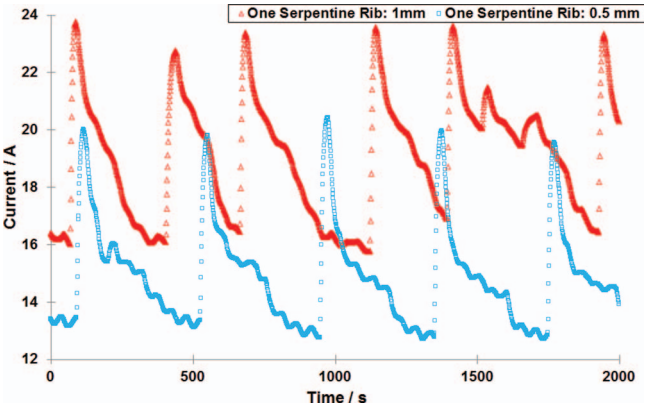

Figure 15. Comparison between configurations (A) and (B) defined in the experimental section under Table I conditions in potentiostatic mode.

current values for configuration 3 due to the differences in the drying process associated with the orientation.

Strong transitions are observed in configurations 1 and 3, where water removal from the channel is inhibited, and no pronounced differences are observed between the two. The transitions are related to the membrane drying and wetting processes associated with the GDL[46] and channel transport properties. Therefore, previous work on the gravitational effect[47,48] has not caused effects on the internal MEA structure. However, whether the membrane thickness has an effect on the transition time remains to be evaluated.

Effect of the flow field on transient response.— The study and design of the bipolar plates have been a challenge and one of the main focuses in the development of PEMFC technology.[49] Different design features and channel configurations in the bipolar plate have been proposed in the literature.[50–52] Earlier work was aimed at studying the effect of the relationship between the rib and channel.[53,54]

In comparing the oscillating behavior of one and five serpentine channels as well as different rib thicknesses, the selected configuration corresponds to case one in Figure 2, as pronounced oscillatory behavior is observed.

In this section, the effect of using bipolar plates with two different rib size thicknesses is analyzed. Figure 15 presents the results of using two different thickness, 0.5 mm and 1 mm, corresponding to configurations A and B specified in the experimental section.

According to the work reported by Reum et al.,[54] a lower response is observed for the thin rib. However, as observed in Figure 15, the oscillatory behavior is not significantly different for these cases. No significant changes in transition times or amplitudes are observed; however, the reported total cell performance effect could be reproduced. Hence, we conclude that the rib thickness has no significant effect on the oscillatory phenomenology.

Next, we discuss the differences in the oscillatory response when bipolar plates with flow field configurations with one or five serpentines are used, corresponding respectively to configurations B and C in the experimental section.

Figure 16 demonstrates that using five serpentines in the bipolar plate reduces the oscillation amplitude and somewhat increases the transition frequency. In addition, the high-performance level is reduced with the five serpentine flow field, indicating that the hydration level of the membrane is reduced. Apparently, the blocking effect of liquid water has a reduced significance for a multiple channel geometry. Therefore, this observation is in accordance with the above interpretation of the importance of forced water convection through the cell.

Furthermore, it must be considered that differences in amplitudes, and especially the low performance level in Figure 16, are associated with differences in the gas velocity in the channel. Five serpentines at

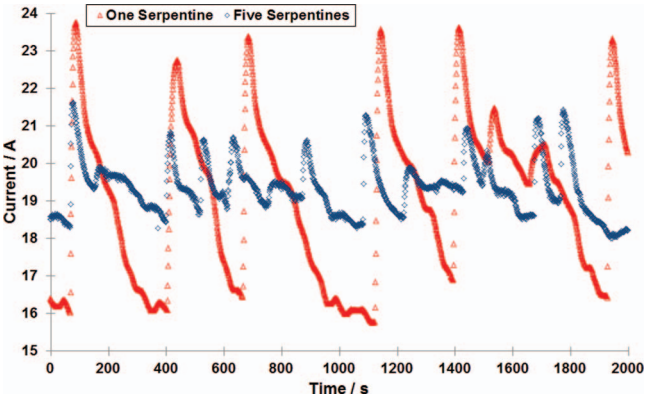

Figure 16. Comparison between configurations (B) and (C) defined in the experimental section under Table I conditions in potentiostatic mode; flow rates of configuration (B), anode: 209 mL/min, cathode: 664 mL/min; flow rates of configuration (C), anode: 42 mL/min, cathode: 133 mL/min.

the cathode also reduces the air drying capacity of the cell. Flow rates are provided in the figure caption.

A final statement relates to the occurrence of oscillations in stacks with cells of 142 cm^2 with multiple serpentine flow fields and carbon composite bipolar plates under comparable conditions. Thus, even if the normal operation conditions vary from the ones for the oscillatory behavior, it is obvious that the extracted information regarding water transport and distribution is of relevance in practical systems.

Conclusions

This study describes the oscillatory response of a single polymer electrolyte fuel cell under different operation modes, namely potentiostatic versus galvanostatic modes, and the effect of cell orientation in the gravity field on the transient behavior. Oscillations appear both under galvanostatic and potentiostatic operation, and the results can be rationalized assuming a liquid water reservoir and changing water fluxes to the cathode due to distinct water-content-dependent electro-osmotic drag rates and permeation rates (corresponding to liquid-vapor permeation). Gravitation naturally does not cause a pronounced effect on the membrane (MEA) drying or wetting process but has a significant effect on the water phase condition in the channels and on the liquid water removal process. Liquid water in the channel leads to pressure buildup and to forced convection of water through the cell. This effect has been identified as a trigger for the upward transition. Consequently, cell orientations affecting the liquid water buildup in the channel have a strong effect on the oscillatory behavior.

The rib size variation significantly affects the performance of the cell but does not have a pronounced effect on the oscillatory behavior. This process is more dependent on other features, such as channel thickness, GDL and flow field design.

Under the same working conditions, with high RH values on both sides, the multi-serpentine flow field cell exhibits reduced performance compared with a single serpentine cell; however, under dehydrated conditions with gradients of humidity between the anode and cathode configuration, a more stable response is observed. Therefore, the flow design of the bipolar plate affects the oscillatory behavior because the channel blocking and gas velocities are strongly affected.

Higher flow rates of wet gases are more effective in improving the stability of the cell response than using larger levels of RH under the same net water amounts. This result is a consequence of the better distribution of the humidity within the cell, with the latter being an essential factor in the wetting and drying process.

Consequently, this work demonstrates that the optimal configuration to work under low-humidity conditions is configuration 2, which is based on a multi-serpentine layout and favors higher flows rates than the higher relative humidities of the anode gas. This work has identified the forced convection of water as an essential process for explaining the occurrence of periodic transitions, which is essential for establishing a realistic transient model of the cell.

Acknowledgments

The authors wish to acknowledge the Deutsche Akademische Austausch Dienst (DAAD), Scholarship code number A/11/94356. The authors would also like to thank H. Sander at DLR and P. Garcia-Ibarra at the Dept. Fisica Matematica y de Fluidos (UNED) for suggestions and discussions.

References

1. R. Hanke-Rauschenbach, M. Mangold, and K. Sundmacher, *Rev. Chem. Eng.*, **27**, 23 (2011).
2. R. Hanke-Rauschenbach, M. Mangold, and K. Sundmacher, *J. Electrochem. Soc.*, **155**, B97 (2008).
3. D. Chen, W. Li, and H. Peng, *J. Power Sources*, **180**, 461 (2008).
4. H. Sun, G. Zhang, L. J. Guo, S. Dehua, and H. Liu, *J. Power Sources*, **168**, 400 (2007).
5. M. M. Nasef and A. A. Aly, *Desalination*, **287**, 238 (2012).
6. R. Lin, C. Cao, J. Ma, E. Gülzow, and K. A. Friedrich, *Int. J. Hydrogen Energy*, **37**, 3373 (2012).
7. L. A. M. Riascos, *J. Power Sources*, **184**, 204 (2008).
8. G. H. Guvelioglu and H. G. Stenger, *J. Power Sources*, **163**, 882 (2007).
9. D. Hyun and J. Kim, *J. Power Sources*, **126**, 98 (2004).
10. Y. Hiramitsu, H. Sato, H. Hosomi, Y. Aoki, T. Harada, Y. Sakiyama, Y. Nakagawa, K. Kobayashi, and M. Hori, *J. Power Sources*, **195**, 435 (2010).
11. D. G. Sanchez, D. G. Diaz, R. Hiesgen, I. Wehl, and K. A. Friedrich, *J. Electroanal. Chem.*, **649**, 219 (2010).
12. K. Jiao and X. Li, *Prog. Energ. Combust.*, **37**, 221 (2011).
13. Q. Duan, H. Wang, and J. Benziger, *J. Membrane Sci.*, **392–393**, 88 (2012).
14. M. Adachi, T. Navessin, Z. Xie, F. H. Li, S. Tanaka, and S. Holdcroft, *J. Membrane Sci.*, **364**, 183 (2010).
15. N. S. Mat Hassan, W. R. Wan Daud, K. Sopian, and J. Sahari, *J. Power Sources*, **193**, 249 (2009).
16. S. Hamel and L. G. Fréchette, *J. Power Sources*, **196**, 6242 (2011).
17. M. V. Williams, H. R. Kunz, and J. M. Fenton, *J. Power Sources*, **135**, 122 (2004).
18. C. I. Lee and H. S. Chu, *J. Power Sources*, **161**, 949 (2006).
19. E. Hontañon, M. J. Escudero, C. Bautista, P. L. Garcia-Ybarra, and L. Daza, *J. Power Sources*, **86**, 363 (2000).
20. S. Dutta, S. Shimpalee, and J. W. Van Zee, *J. Appl. Electrochem.*, **30**, 135 (2000).
21. Y. Wang and C. Y. Wang, *Electrochim. Acta*, **51**, 3924 (2006).
22. D. H. Jeon, K. N. Kim, S. M. Baek, and J. H. Nam, *Int. J. Hydrogen Energ.*, **36**, 12499 (2011).
23. T. C. Yau, M. Cimenti, X. Bi, and J. Stumper, *J. Power Sources*, **196**, 9437 (2011).
24. Y. Lee, B. Kim, and Y. Kim, *Int. J. Hydrogen Energ.*, **34**, 1999 (2009).
25. H. K. Hsuen and K. M. Yin, *Electrochim. Acta*, **62**, 447 (2012).
26. H. Fukumoto, H. Maeda, and K. Mitsuda, *Denki Kagaku oyobi Kogyo Butsuri Kagaku*, **68**, 794 (2000).
27. J. R. Atkins, S. C. Savett, and S. E. Creager, *J. Power Sources*, **128**, 201 (2004).
28. D. G. Sanchez and P. L. Garcia-Ybarra, *Int. J. Hydrogen Energ.*, **37**, 7279 (2012).
29. J. Benziger, E. Chia, J. F. Moxley, and I. G. Kevrekidis, *Chem. Eng. Sci.*, **60**, 1743 (2005).
30. I. Nazarov and K. Promislow, *Chem. Eng. Sci.*, **61**, 3198 (2006).
31. X. D. Wang, Y. Y. Duan, W. M. Yan, and X. F. Peng, *Electrochim. Acta*, **53**, 5334 (2008).
32. W. H. J. Hogarth and J. B. Benziger, *J. Power Sources*, **159**, 968 (2006).
33. X. D. Wang, W. M. Yan, W. C. Won, and D. J. Lee, *Int. J. Hydrogen Energ.*, **37**, 15808 (2012).
34. Y. C. Park, P. Chippar, S. K. Kim, S. Lim, D. H. Jung, H. Ju, and D. H. Peck, *J. Power Sources*, **205**, 32 (2012).
35. E. Gulzow, M. Schulze, N. Wagner, T. Kaz, R. Reissner, G. Steinhilber, and A. Schneider, *J. Power Sources*, **86** 352 (2000).
36. M. Schulze, E. Gulzow, S. Schonbauer, T. Knori, and R. Reissner, *J. Power Sources*, **173**, 19 (2007).
37. S. J. C. Cleghorn, C. R. Derouin, M. S. Wilson, and S. Gottesfeld, *J. Appl. Electrochem.*, **28**, 663 (1998).
38. D. J. L. Brett, S. Atkins, N. P. Brandon, V. Vesovic, N. Vasileiadis, and A. R. Kucernak, *Electrochem. Commun.*, **3**, 628 (2001).
39. J. Stumper, S. A. Campbell, D. P. Wilkinson, M. C. Johnson, and M. Davis, *Electrochim. Acta*, **43**, 3773 (1998).
40. Z. Lu, S. G. Kandlikar, C. Rath, M. Grimm, W. Domigan, A. D. White, M. Hardbarger, J. P. Owejan, and T. A. Trabold, *Int. J. Hydrogen Energ.*, **34**, 3445 (2009).
41. S. Ge and C. Y. Wang, *J. Electrochem. Soc.*, **154**, B998 (2007).
42. K. Tüber, D. Pocza, and C Hebling, *J. Power Sources*, **124**, 403 (2003).
43. J. Eller, T. Rosen, F. Marone, M. Stampanoni, A. Wokaun, and F. N. Büchi, *J. Electrochem. Soc.*, **158**, B963 (2011).
44. Z. Lu, C. Rath, G. Zhang, and S. G. Kandlikar, *Int. J. Hydrogen Energ*, **36**, 9875 (2011).
45. S. Dusan and K. Ajay, *J. Power Sources*, **170**, 334 (2007).

46. Z. Lu, M. M. Daino, C. Rath, and S. G. Kandlikar, *Int. J. Hydrogen Energ*, **35**, 4233 (2010).
47. F. Y. Zhang, X. G. Yang, and C. Y. Wang, *J. Electrochem. Soc.*, **153**, A225 (2006).
48. C. E. Colosqui, M. J. Cheah, I. G. Kevrekidis, and J. B. Benzinger. *J. Power Sources*, **196**, 10057 (2011).
49. J. P. Owejan, J. J. Gagliardo, J. M Sergi, S. G. Kandlikar, and T. A. Trabold, *Int. J. Hydrogen Energ.*, **34**, 3436 (2009).
50. X. Li and I. Sabir, *Int. J. Hydrogen Energ.*, **30**, 359 (2005).
51. C. Xu and T. Zhao, *Electrochem. Commun.*, **9**, 497 (2007).
52. S. M. Senn and D. Poulikakos, *J. Power Sources*, **130**, 178 (2004).
53. M. Reum, A. Wokaun, and F. Büchi, *J. Electrochem. Soc.*, **156**, B1225 (2009).
54. M. Reum, A. Wokaun, and F. Büchi, *J. Electrochem. Soc.*, **157**, B673 (2010).